ELSEVIER

International Journal of Fatigue 22 (2000) 217–228

International Journal of Fatigue

www.elsevier.com/locate/ijfatigue

Low cycle fatigue analysis of temperature and frequency effects in eutectic solder alloy

X.Q. Shi [a,*], H.L.J. Pang [b], W. Zhou [b], Z.P. Wang [a]

[a] *Gintic Institute of Manufacturing Technology, Nanyang Drive, Singapore 638075, Singapore*
[b] *School of Mechanical and Production Engineering, Nanyang Technological University, Singapore 639798, Singapore*

Received 23 August 1999; received in revised form 19 November 1999; accepted 19 November 1999

Abstract

Low cycle isothermal mechanical fatigue testing of a eutectic alloy 63Sn/37Pb was carried out in a systematic manner over a wide range of frequencies (10^{-4}–1 Hz) and temperatures (−40 to 150°C) with the total strain set at different values (1–50%). The low cycle fatigue behavior of the eutectic solder was found to be strongly dependent on test temperature and frequency. If the Coffin–Manson model is used to describe such fatigue behavior, the fatigue exponent m and ductility coefficient C in the model are found to be a function of temperature and frequency rather than numerical constants. The plastic flow law was employed to explain the temperature and frequency dependence. The frequency-modified Coffin–Manson model was tried and found to be able to eliminate the frequency dependence of the numerical "constants" but not the temperature dependence. To have a full description of the temperature- and frequency-dependent fatigue behavior, a set of empirical formulae was derived based on the frequency-modified Coffin–Manson model. © 2000 Elsevier Science Ltd. All rights reserved.

Keywords: Low cycle fatigue; Eutectic solder; Temperature and frequency dependent; Plastic flow law; Frequency-modified Coffin–Manson

1. Introduction

Eutectic solder alloys are commonly used in surface mount technology (SMT) soldering processes to form solder interconnections which serve as electrical and mechanical connections between the electronic component and the printed circuit board (PCB). During service load conditions, the coefficient of thermal expansion mismatch between the component and the board, caused by power and environmental temperature changes, generates thermally induced strains in the solder joints leading to thermal fatigue failures. Low cycle fatigue failure of solder joints due to the thermal mismatch strain is recognized as a major cause of failure in surface mounted electronic devices. Therefore, it is important to understand the low cycle fatigue behavior of solder alloy in order to improve the long-term reliability of SMT solder joints in PCBs.

Thermal fatigue experiments are difficult to study because they are time-consuming and require special thermal cycling equipment and test facilities. Furthermore, the studies are made difficult due to the changing material properties of solder as the temperature changes during thermal fatigue loading [1]. An approach to this problem is to investigate the fatigue behavior of solder joints using isothermal mechanical fatigue tests. This has led to considerable research efforts in trying to model the fatigue behavior of low cycle fatigue life prediction models for solder joints.

In general, three types of specimens have been used to study the fatigue behavior of solder and they are actual SMT solder joint specimens, simplified shear specimens, and bulk solder test samples. Much work has been done on actual SMT solder joint specimens, ranging from leaded chip carrier printed circuit boards [2–4] to leadless chip carrier printed circuit boards [5,6]. This approach has the advantage of testing the solder joints of actual electronic components, but the main disadvantage is that the results are specific to the components used and are not easily applied to other applications. Simplified shear specimens are usually fabricated from two pieces of metal plates joined by solder. Different

* Corresponding author. Tel.: +65-790-5514; fax: +65-791-1859.
E-mail address: mhlpang@ntu.edu.sg (H.L.J. Pang).

0142-1123/00/$ - see front matter © 2000 Elsevier Science Ltd. All rights reserved.
PII: S0142-1123(99)00124-3

types of simplified shear specimens have been used in different laboratories [7–12]. Some examples are the single shear specimen, double shear specimen, lap-shear specimen, and ring-pin specimen. These investigations make good contributions to the understanding of solder joint fatigue reliability. However, since the stress–strain distribution in these SMT solder joint specimens and simplified shear specimens gives rise to a complex multiaxial stress–strain state, the reported test results should be used with caution. The reported test results may represent the fatigue behavior of the structure or test specimen rather than that of the solder material itself [13]. In bulk solder sample tests, a pure tension or pure shear stress–strain state is preferred. Therefore, fatigue data of bulk solder samples are needed to provide a firm basis for fundamental low cycle fatigue studies and to provide further understanding of the fatigue failure behavior over a wide range of test temperatures and test frequencies. For example, Jiang [14] gave the fatigue data of 60Sn/40Pb solder alloy at room temperature for a certain strain rate (3.3×10^{-3} s^{-1}). Hence more low fatigue test data at different temperatures and frequencies is required.

Service temperature changes seldom ramp up and then ramp down as rapidly as is found in thermal cycling tests. Rather, the temperature is held constant for a period of time before changing. In the case of real service joints this hold time may be a matter of hours, a day, or even longer. Eutectic solder is a low-melting point alloy (183°C for 63Sn/37Pb); the environmental temperature often simulated in accelerated thermal cycling tests can vary from −40 to 125°C and is about 0.5–0.85 times T_m (melting point) of the eutectic solder alloy. At such high homologous temperatures, the thermal fatigue process must be accompanied with creep. The creep contribution to fatigue failure changes as the hold time or cyclic frequency is changed during service loads or during reliability tests. Obviously, low cycle fatigue data used for solder joint reliability assessments must account for the cyclic frequency effects at different service load or reliability test load conditions. Isothermal mechanical fatigue tests are often used instead of thermal cycling fatigue tests to study the low cycle fatigue behavior of solder at different test temperatures and frequencies. In this paper, a low cycle fatigue test program for 63Sn/37Pb eutectic solder alloy was carried out in a systematic manner over a wide range of test frequencies of 10^{-4}–1 Hz, and test temperatures from −40 to 150°C, under total strain control conditions set at different values of a 1–50% total strain range. The test results developed were analysed using low cycle fatigue models where the effects of temperature and frequency have been accounted for in a frequency-modified Coffin–Manson model with temperature-dependent constants.

2. Experimental details and procedures

The fatigue specimens used in the tests were cylindrical specimens with a gauge length of 50 mm and a central diameter of 6 mm, as shown in Fig. 1. A large radius of curvature of 105 mm was made in the gauge section to prevent any stress concentration due to sharp corners. The specimens were machined from high purity 63Sn/37Pb solder bars in the as-cast condition. The solder contained 63wt% Sn and 37wt% Pb. After machining, the gauge section of each specimen was carefully ground on fine SiC paper and polished using 1 μm diamond paste. Afterwards, the fatigue specimens were annealed at 60°C for 24 h in a N_2 atmosphere to eliminate the residual stresses.

The fatigue tests were conducted on a servo-valve-controlled electro-hydraulic testing machine from MTS (model 810). The gripping device of the machine was designed in such a way that only a small gripping load was required to grip the soft solder specimens. The machine has the capacity to produce very low frequencies in the wide range 10^{-4}–1 Hz. The tests were run under a symmetrical uniaxial tension–compression loading with total strain control. The triangular waveform was employed for all the fatigue tests. The total strain was measured using a dynamic extensometer which was attached to the specimen within the gauge length. The testing was carried out at five different frequencies (10^{-4}, 10^{-3}, 10^{-2}, 10^{-1}, and 1 Hz) and at five different temperatures (−40, 25, 75, 125, and 150°C) with total strain set at six different values (1, 2, 5, 10, 25, and 50%). For each test condition at least six specimens were used. The number of cycles to failure for each of the specimens was recorded as the fatigue life.

3. Low cycle fatigue test results

3.1. Effect of plastic strain range on low cycle fatigue

A large number of fatigue tests were carried out using various combinations of testing parameters. Generally, scatter in fatigue life of the solder tested using the same parameters (i.e. the same temperature, frequency and total strain range) was found to be small, as illustrated in Fig. 2. The small scatter makes it easy to observe the effect of a certain testing parameter on fatigue life. For example, Fig. 2 shows clearly that fatigue life of the solder decreases with increasing total strain range at a given temperature and frequency. In the present research, at least six specimens were tested for each of the test conditions and the average fatigue life is used in the following analyses.

The Coffin–Manson model [15,16] has been widely used to predict low cycle fatigue life N_f of most metallic

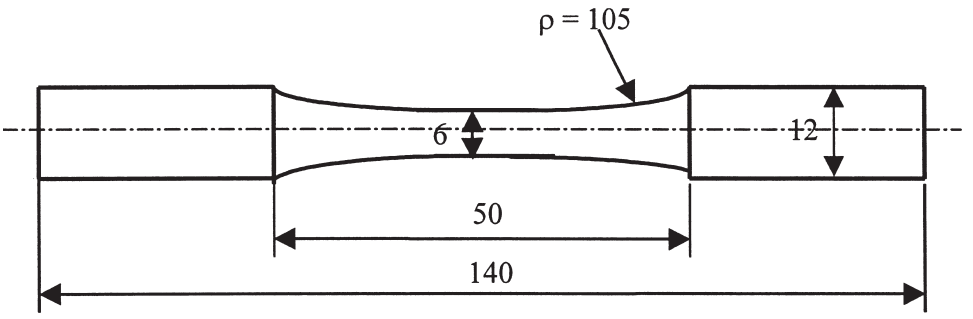


Fig. 1. Geometry of fatigue specimen (unit: mm).

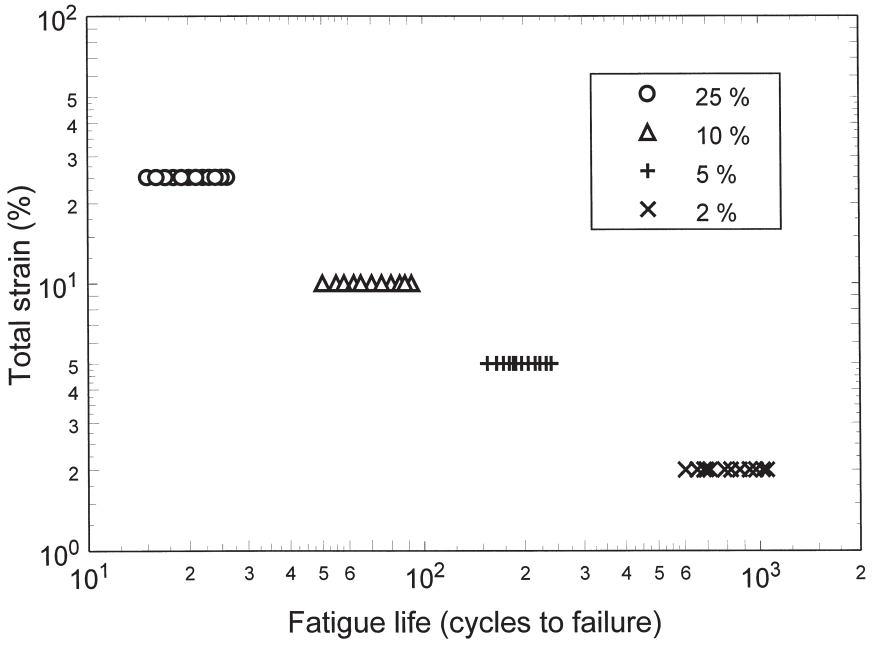


Fig. 2. Total strain range versus fatigue life at 25°C and 1 Hz.

materials in terms of the plastic strain range $\Delta\varepsilon_p$, as shown below:

$$N_f^m \Delta\varepsilon_p = C \quad (1)$$

where m and C are numerical constants. Some studies have found that the low cycle fatigue behavior of solder alloy can be modeled using the Coffin–Manson relationship [17–19]. Using the hysteresis loop, the plastic strain can be obtained by taking the intercept of the loop on the strain axis [20]. The relationship between the plastic strain and mean fatigue life is presented on log–log scales in Fig. 3. It is noted that the fatigue life has a good linear relationship with the plastic strain in the 1–50% total strain range. The fatigue exponent m and ductility coefficient C are equal to 0.736 and 2.05, respectively. It is concluded, therefore, that the Coffin–Manson relationship is applicable to the low cycle fatigue behavior of 63Sn/37Pb solder at a temperature of 25°C. The effect of test temperature and frequency on the low cycle fatigue behavior of solder is reported in the following sections.

3.2. Effect of temperature on low cycle fatigue behavior

A series of repeated tests at the same frequency and total strain but at different environmental temperatures was conducted. The fatigue life was found to decrease linearly with increasing temperature for a test frequency of 1 Hz, as shown in Fig. 4. The effect of lower test frequency (i.e. below 1 Hz) will be discussed in the next section. Since the fatigue life is a function of temperature, the numerical constants in the Coffin–Manson model must be determined for different environmental temperatures.

The relationship between the mean fatigue life and plastic strain obtained from tests at five different temperatures (−40, 25, 75, 125, and 150°C) is presented in Fig. 5. From Fig. 5, the values of constants m and C for the Coffin–Manson model can be determined for different temperatures by taking the slope and the intercept on the plastic strain axis. The results are plotted in Fig. 6. It can be seen that the m value decreases with increasing

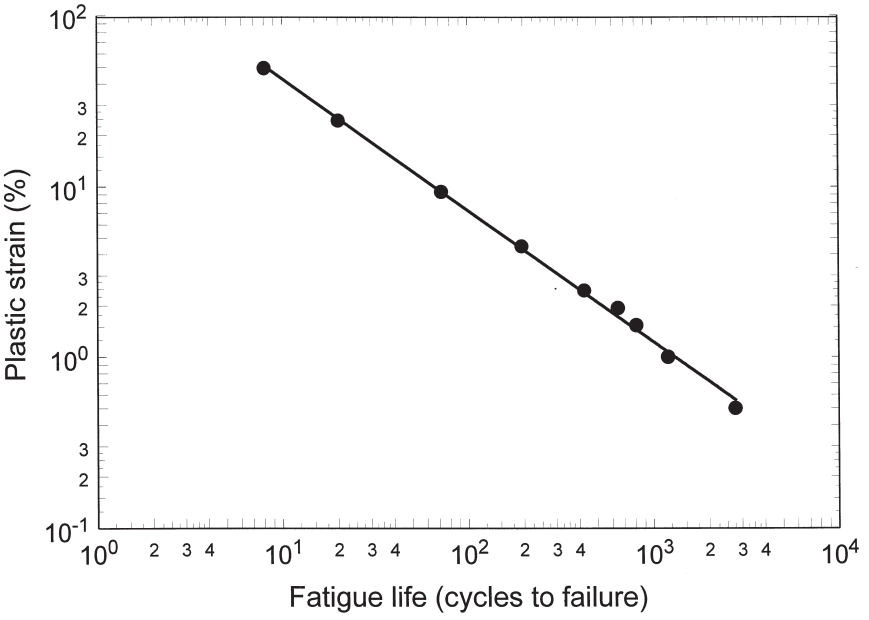


Fig. 3. Plastic strain range versus fatigue life at 25°C and 1 Hz.

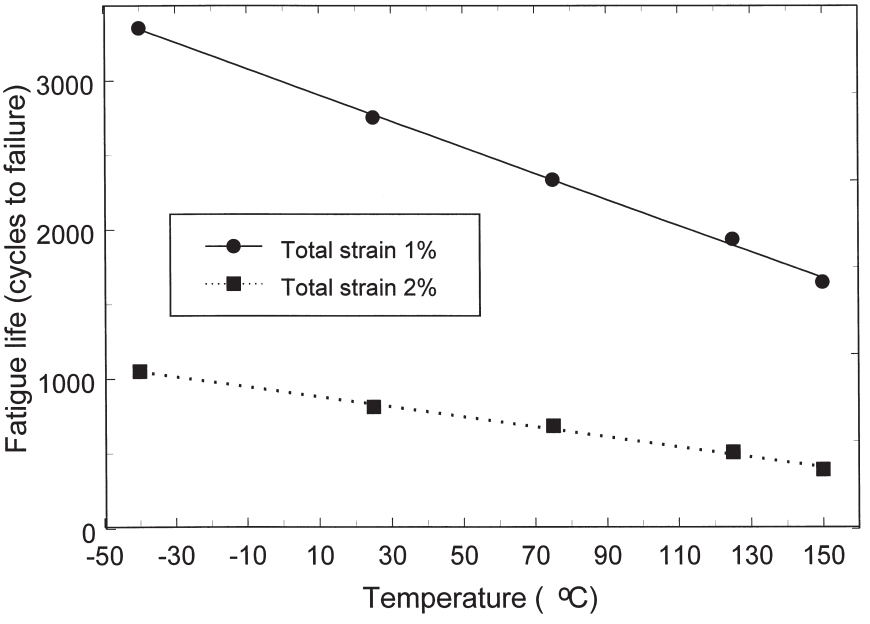


Fig. 4. Fatigue life versus temperature at 1 Hz for two total strain levels.

temperature, but the temperature dependence is small from 0.763 at −40°C to 0.69 at 150°C. In contrast, the C value decreases distinctly with increasing temperature from 2.75 at −40°C to 0.98 at 150°C.

The temperature variation of the material fatigue exponent m in the Coffin–Manson model can be understood by considering the deformation behaviors of the solder. As shown in Fig. 7, the area of the hysteresis loop, which represents the energy dissipation, decreases with increasing temperature for a given frequency and strain range. In Fig. 8, it decreases with decreasing frequency for a given strain range and temperature. The slight asymmetry of the hysteresis loop is affected by the material hardening under the tensile loading and softening under the compression loading.

According to a plastic flow law relationship [21], the applied stress range $\Delta\sigma$, plastic strain range $\Delta\varepsilon_p$, and plastic strain rate $\dot{\varepsilon}_p$ can be defined as follows:

$$\Delta\sigma = A\Delta\varepsilon_p^{\alpha}\dot{\varepsilon}_p^{\beta} \tag{2}$$

where A, α, and β are numerical constants. For fatigue

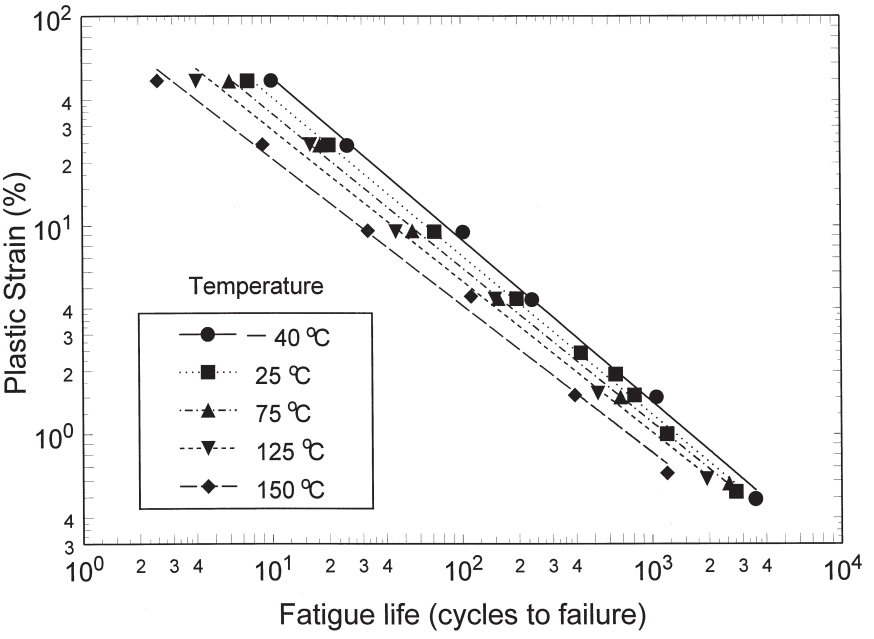


Fig. 5. Plastic strain versus fatigue life at 1 Hz for different temperatures.

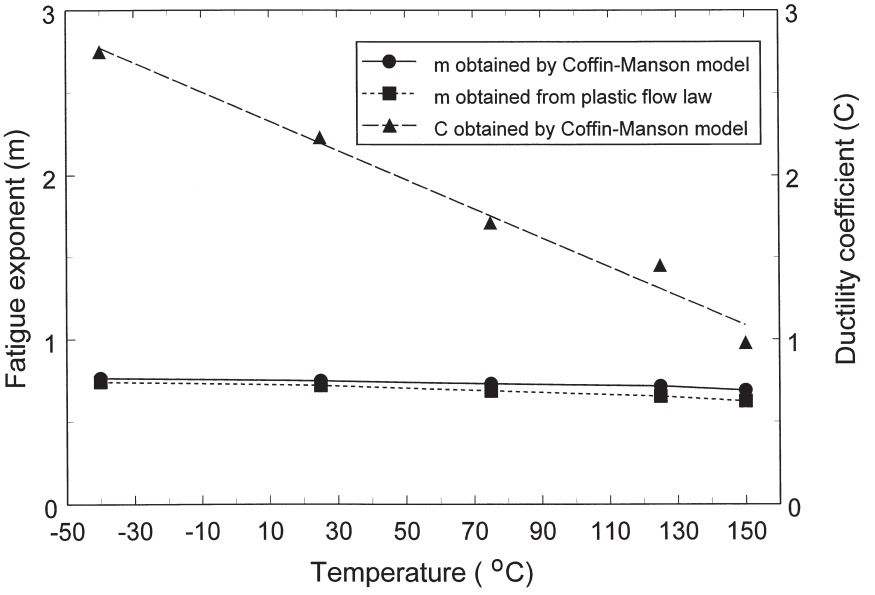


Fig. 6. Constants m and C as a function of temperature at 1 Hz.

tests carried out at constant cycling frequency ν, Eq. (2) becomes

$$\Delta\sigma = A'\Delta\varepsilon_p^{\alpha}\nu^{\beta} \tag{3}$$

where A' is a numerical constant. When frequency ν is constant, Eq. (3) can be rewritten as

$$\alpha = \left(\frac{\Delta \log \Delta\sigma}{\Delta \log \Delta\varepsilon_p}\right)_{\nu} \tag{4}$$

By plotting the curves of the applied stress range $\Delta\sigma$ versus plastic strain range $\Delta\varepsilon_p$ at the fixed frequency (1 Hz), as shown in Fig. 9, the slope of each curve, which represents the material cyclic strain hardening exponent α at a given temperature condition, can be obtained. Based on the energy dissipated during the fatigue cycling, Morrow [22] has pointed out that the value of m is related to the cyclic strain hardening exponent α in the following formula:

$$m = \frac{1}{1+5\alpha} \tag{5}$$

Substituting the values of α into Eq. (5), the values

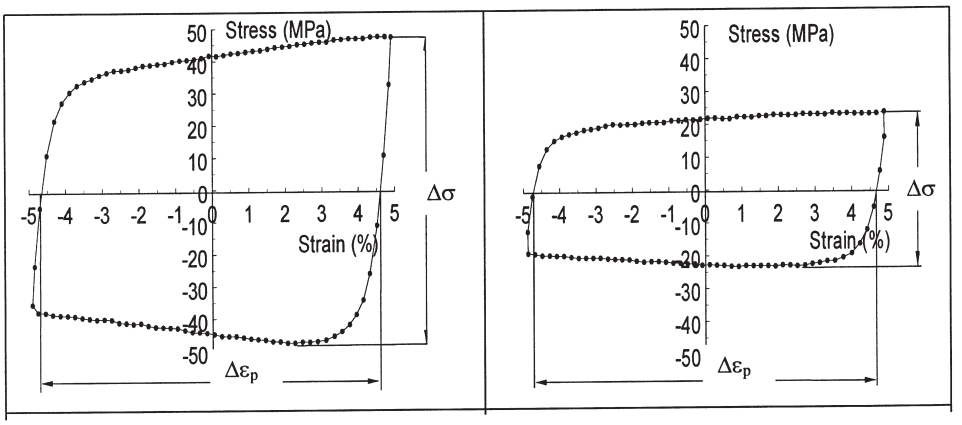


Fig. 7. Hysteresis loops at 1 Hz and strain range of 10%: effect of temperature at (a) 25°C, and (b) 150°C.

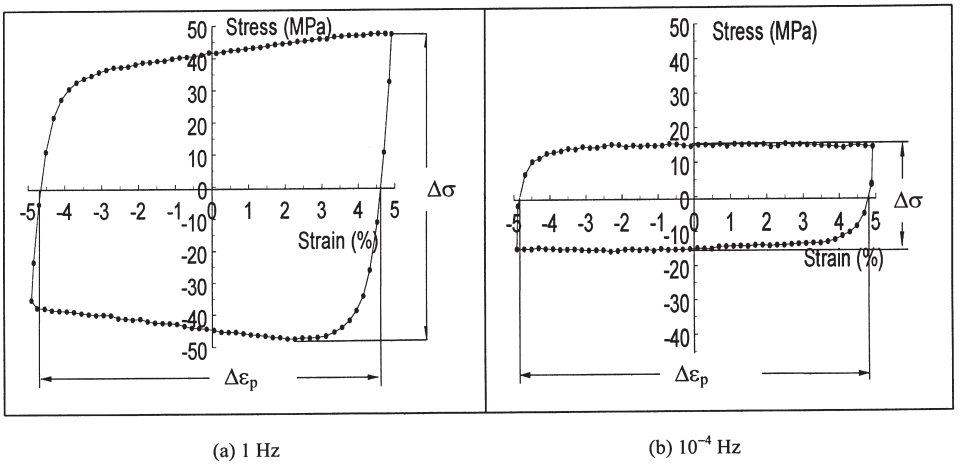


Fig. 8. Hysteresis loops at 25°C and strain range of 10%: effect of frequencies at (a) 1 Hz, and (b) 10^{-4} Hz.

of fatigue exponent m can be obtained as a function of temperature, as shown in Fig. 6. It is clear that the m values obtained by the plastic flow law tend to decrease slightly with increasing temperature, and this is in good agreement with the results obtained from the Coffin–Manson data shown in Fig. 5.

Since the value of m tends to decrease slightly with increasing temperature and the fatigue life N_f also decreases with increasing temperature as shown in Fig. 4, the material ductility coefficient C in the Coffin–Manson equation, which is proportional to N_f^m, is expected to decrease with increasing temperature. This explains well the observed temperature dependence of C, as shown in Fig. 6.

3.3. Effect of frequency on low cycle fatigue behavior

In this section, the low cycle fatigue behavior of the eutectic solder at different frequencies (10^{-4}–1 Hz) is analyzed. As shown in Fig. 10, the fatigue life of the solder decreases with decreasing frequency, but the curve of fatigue life versus frequency displays a double-linear characteristic. When frequency is above 10^{-3} Hz, the linear slope is small, and the fatigue life is weakly dependent on frequency. However, when frequency is reduced to below 10^{-3} Hz, the fatigue life decreases drastically.

The double-linear characteristic of fatigue life can be attributed to accumulated creep damage during fatigue testing. As the frequency decreases, the time to failure increases, and this allows more time for creep to develop and thus leads to lower fatigue life in terms of cycles to failure. At a frequency above 10^{-3} Hz, absolute time increment change is small as frequency is reduced by one order of magnitude, for example from 1 to 0.1 Hz; therefore, creep damage during fatigue decreases weakly with decreasing frequency. However, when frequency is reduced from 10^{-3} to 10^{-4} Hz, the time to failure increases drastically and this results in a larger decrease in fatigue life. It should be noted that the increase in time to failure when frequency is reduced by one order of magnitude from 10^{-3} to 10^{-4} Hz is approximately 10

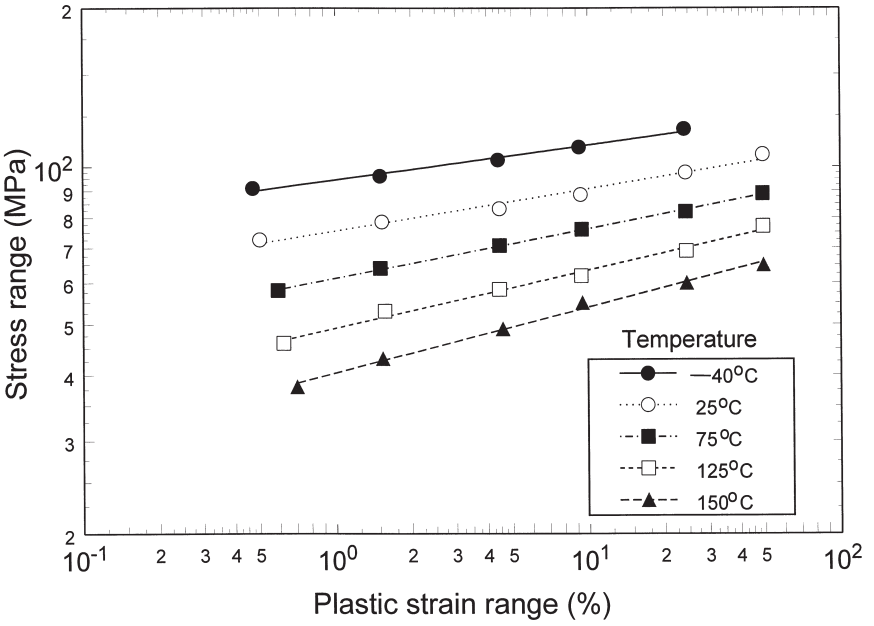


Fig. 9. Applied stress range versus plastic strain range at 1 Hz for different temperatures.

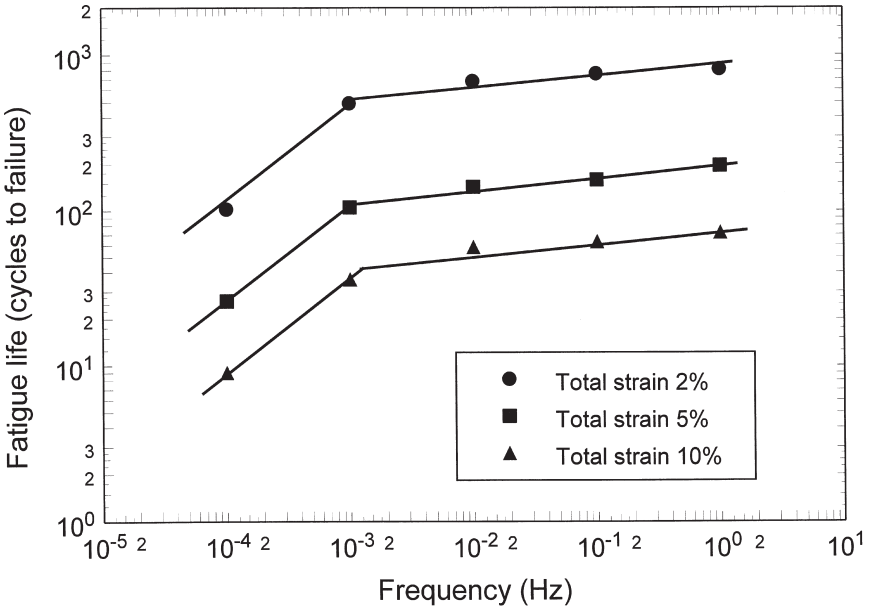


Fig. 10. Relationship between fatigue life and frequency at the temperature (25°C).

times as large as the failure time increased when frequency is reduced by three orders of magnitude from 1 to 10^{-3} Hz.

As can be seen from Fig. 11, the Coffin–Manson model can be used to describe the fatigue behavior of eutectic solder alloy for any given frequency. However, the fatigue results have large differences at different frequencies, the values of fatigue exponent m and ductility coefficient C change as frequency changes. Based upon the curves of plastic strain against fatigue life, the values of m and C can be obtained by taking the linear slope and the intercept on the plastic strain axis. The results are presented as a function of frequency in Fig. 12. It is noted that the m value decreases gradually with logarithmically decreasing frequency, but the frequency dependence is small. However, the C value decreases significantly as frequency decreases, and is strongly frequency dependent.

Similar to temperature dependence, the frequency variation of the fatigue exponent m in the Coffin–Manson model can be understood by considering the deformation behavior of the solder. Based on Eq. (4), the

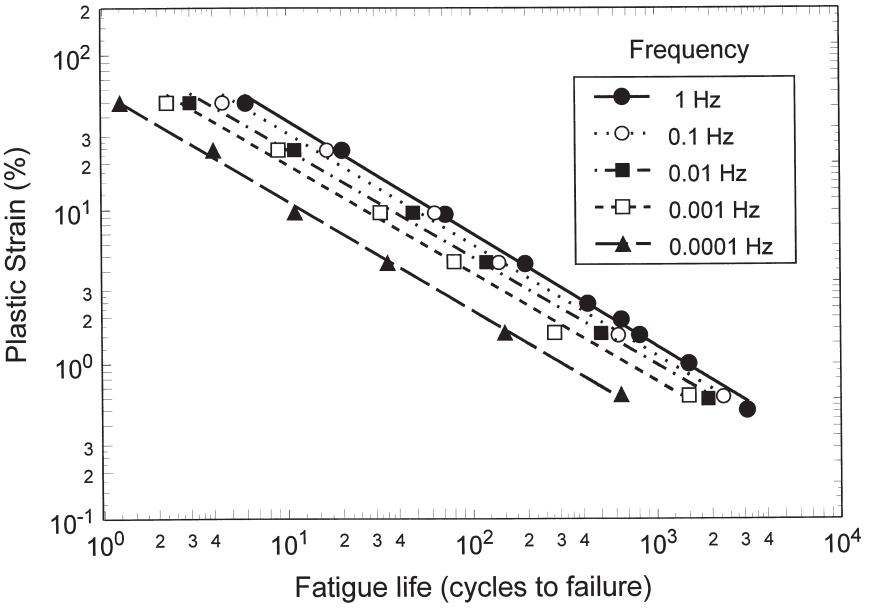


Fig. 11. Plastic strain versus fatigue life at 25°C for different frequencies.

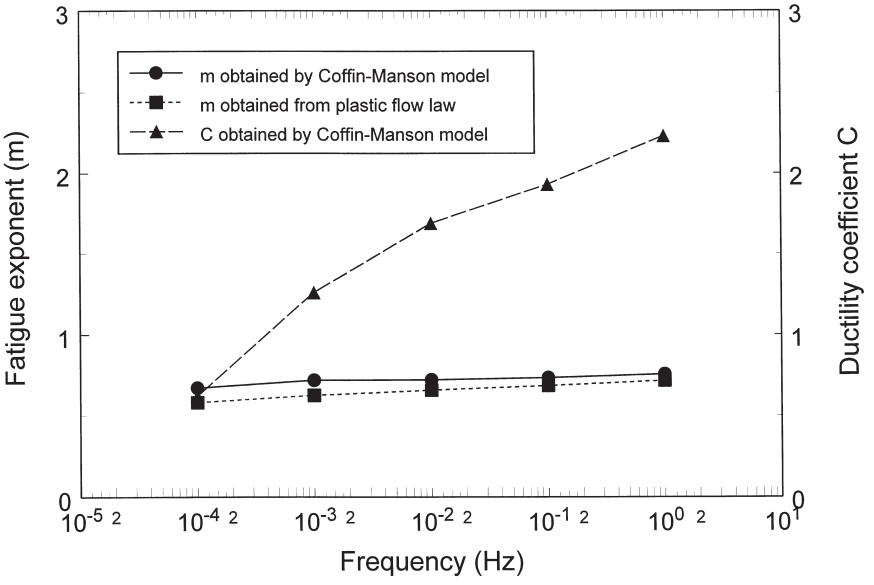


Fig. 12. Constants (m and C) as a function of frequency at 25°C.

relationship between the applied stress range $\Delta\sigma$ and plastic strain range $\Delta\varepsilon_p$, which are obtained from the hysteresis loop, can be plotted for any given frequency, as shown in Fig. 13. It is found that the slope of the curve increases as frequency decreases, and therefore the fatigue exponent m should decrease with decreasing frequency, as shown in Fig. 12. The results are again shown to be very close to those measured from the Coffin–Manson curves in Fig. 11. Fatigue life N_f has an exponential relationship with material ductility coefficient C in the Coffin–Manson model, therefore, when plastic strain range is constant, the C value has a large reduction while the fatigue life N_f and fatigue exponent m have a slight reduction.

3.4. Frequency-modified Coffin–Manson relationship

To consider the interaction between creep and fatigue, the frequency-modified Coffin–Manson relationship was introduced to describe the low cycle fatigue behavior of eutectic solder [23], given by

$$[N_f \nu^{(k-1)}]^m \Delta\varepsilon_p = C \tag{6}$$

where ν is frequency, k is frequency exponent. When

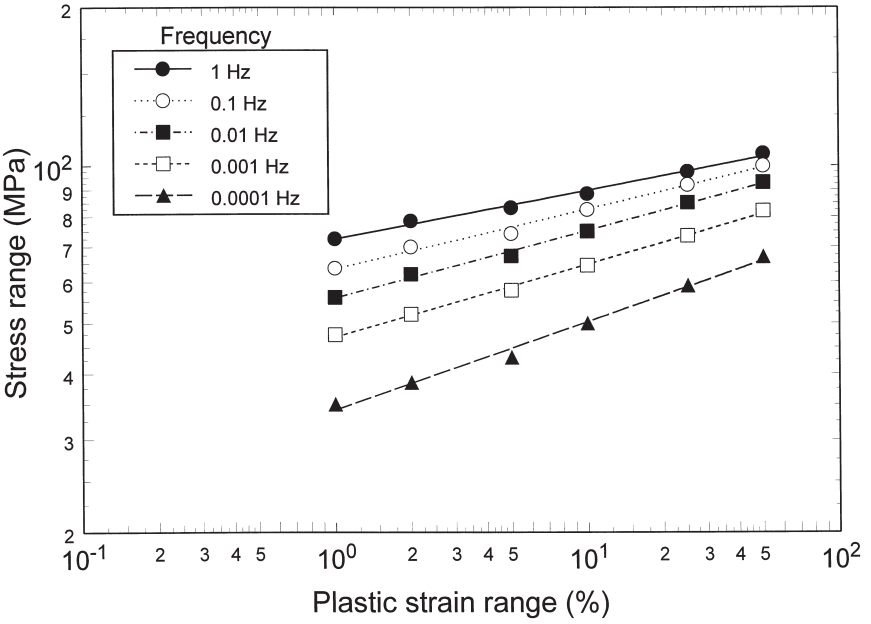


Fig. 13. Applied stress range versus plastic strain range at 25°C for different frequencies.

the plastic strain range is constant, fatigue life N_f has a linear relationship with frequency ν in logarithmic coordinate, and the slope of the curve is the value of $(1-k)$. As shown in Fig. 10, the fatigue life of the solder studied is slightly frequency-dependent for the frequency range from 10^{-3} to 1 Hz, but is strongly frequency-dependent for the lower frequency range from 10^{-3} to 10^{-4} Hz. Therefore, k values were calculated separately in the two frequency ranges and found to be roughly 0.91 and 0.42, respectively, for all the test strain levels.

The characteristic of the k value, at different strain levels, can be understood by Eq. (2). For a certain strain range, Eq. (2) can be written as

$$\beta=\left(\frac{\Delta \log \Delta\sigma}{\Delta \log \dot{\varepsilon}_p}\right)_{\Delta\varepsilon_p} \tag{7}$$

For the fatigue tests at different strain levels, the ramp rate is different, and therefore the strain rate is different. Based upon the hysteresis loop, the applied stress range can be obtained for any given strain range. Meanwhile, the strain rate can be determined from a given strain range and frequency. When the applied stress range is plotted against the strain rate, the data points obtained at a wide range of frequencies (10^{-4}–1 Hz) were found to fit well into a single curve, as shown in Fig. 14. From Eq. (7), it is found that the slope of the curve in Fig. 14 is the value of β. That is to say, the β value does not change as the strain range changes. However, the parameter β is related to frequency and represents the viscous characteristic of the solder deformation. For the constant strain range but at different frequencies, it can be assumed that fatigue life N_f is dominated by the applied stress range

$$N_f \propto \Delta\sigma \tag{8}$$

Substituting Eq. (8) into Eq. (6), the following relationship can be obtained

$$\Delta\sigma \propto C' \Delta\varepsilon_p^{-m} \nu^{(1-k)} \tag{9}$$

It should be noted that Eq. (9) has a similar form compared with Eq. (3), indicating that the frequency exponent k has a linear relationship with the parameter β,

$$(1-k) \propto \beta \tag{10}$$

Hence, the frequency exponent k is independent of strain range.

The k values at the two frequency ranges were used to calculate the frequency modified coefficient $\nu^{(k-1)}$, i.e.

$$\nu^{(k-1)}= \tag{11}$$

$$\begin{cases} \nu^{(k_1-1)} \text{ for } 1 \text{ Hz} \geq \nu \geq 10^{-3} \text{ Hz} \\ \left[\dfrac{\nu}{10^{-3}}\right]^{(k_2-1)} (10^{-3})^{(k_1-1)} \text{ for } 10^{-3} \text{ Hz} > \nu \geq 10^{-4} \text{ Hz} \end{cases}$$

The results were then used to calculate the frequency modified fatigue life $N_f \nu^{(k-1)}$. When the plastic strain was plotted against the frequency-modified fatigue life, all the fatigue life data points obtained at different frequencies were found to fit well into a single curve, as shown in Fig. 15. That is to say, the frequency-modified Coffin–Manson relationship can be used to eliminate the

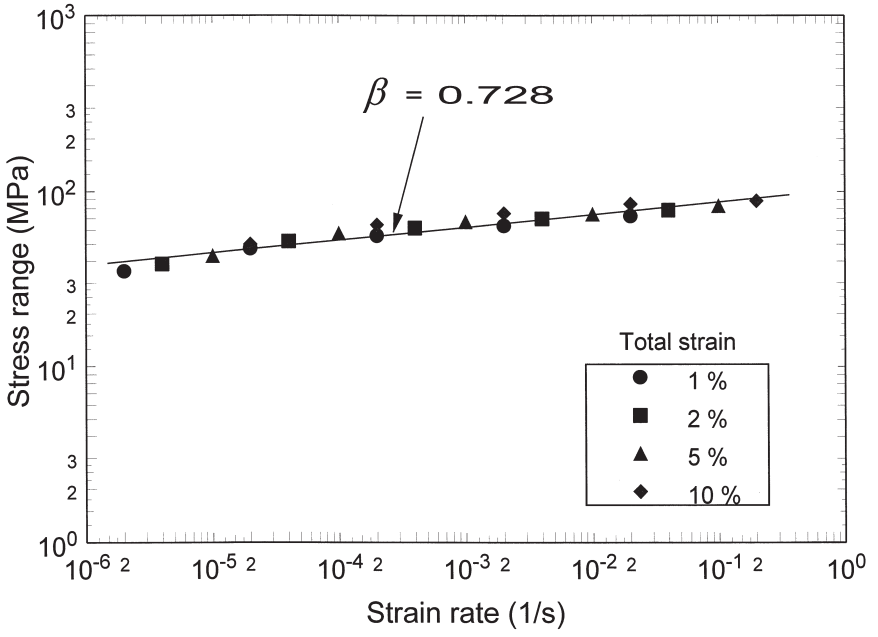


Fig. 14. Stress range versus strain rate at 25°C for different strain levels.

influence of frequency on the low cycle fatigue behavior of 63Sn/37Pb solder.

Furthermore, the frequency-modified Coffin–Manson relationship was used to describe the interaction between fatigue and creep at the other four temperatures (−40, 75, 125, and 150°C). Firstly, based upon the relationship between fatigue life and frequency, the frequency exponents of k_1 and k_2 can be calculated from the two frequency ranges of 10^{-3}–1 Hz and 10^{-4}–10^{-3} Hz, respectively. The results were then plotted as a function of temperature in Fig. 16. It can be seen that the values of k_1 and k_2 decrease with increasing temperature. This shows that the frequency influence is more obvious, and the reduction of fatigue life is larger at higher temperature than that at lower temperature. By substituting these results of k_1 and k_2 into the frequency-modified Coffin–Manson model, the relationship between plastic strain and frequency-modified fatigue life can be obtained at any given temperature. The analysis shows that the frequency-modified Coffin–Manson model can be used to

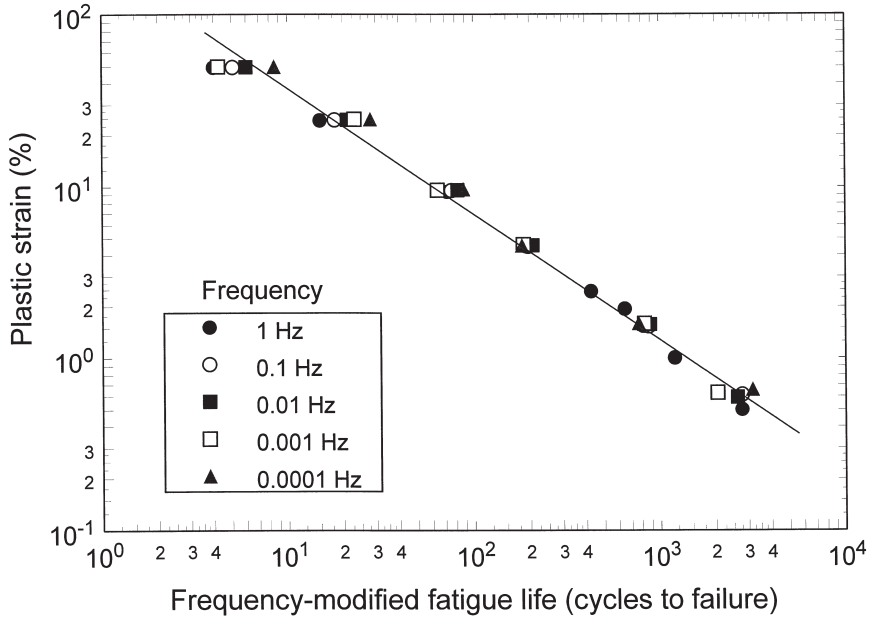


Fig. 15. Plastic strain versus frequency-modified fatigue life at 25°C.

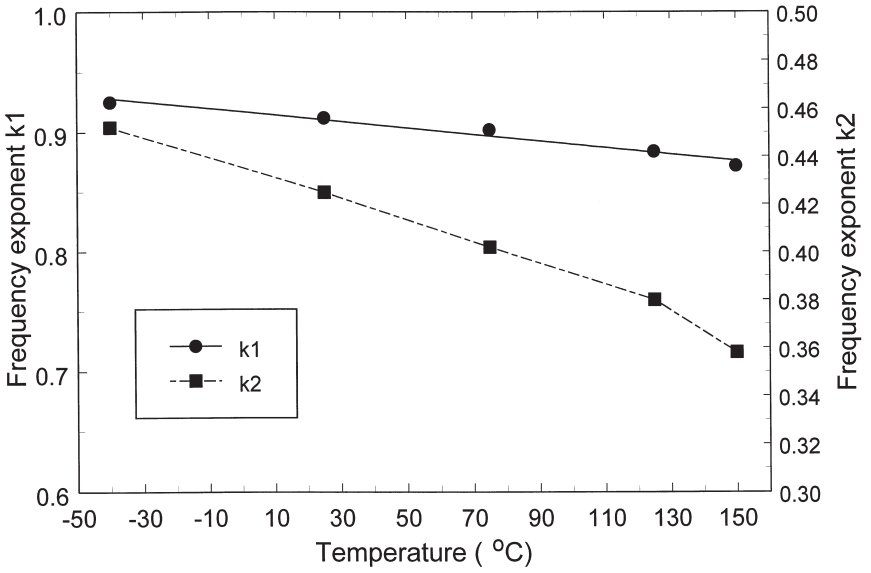


Fig. 16. Frequency exponents (k_1 and k_2) versus temperature.

correlate the fatigue life data for each temperature, but the curves show different slopes and intercepts at different temperatures. As a matter of fact, the parameters (k and v), which are introduced into the frequency-modified Coffin–Manson model, are only frequency-dependent. Therefore, the frequency-modified Coffin–Manson model still cannot be used to eliminate the effect of temperature on values of the numerical parameters k, m, and C. Obviously, it is necessary to introduce a further parameter, which is temperature-dependent, into the frequency-modified Coffin–Manson model [24].

By taking the slope and intercept from the curves at each temperature, the values of m and C can be obtained and plotted as a function of temperature in Fig. 17. Similar to the result obtained at the fixed frequency (1 Hz), the m value decreases slightly as the temperature increases, but the C value still decreases considerably with increasing temperature.

Using the experimental data of k_1, k_2, m, and C given in Figs. 16 and 17, the temperature dependent empirical formulae of the "constants" can be determined by polynomial expression fitting, as follows

$$k_1 = 0.919 - 1.765\times10^{-4}T - 8.634\times10^{-7}T^2 \quad (12a)$$

$$k_2 = 0.437 - 3.753\times10^{-4}T - 8.04\times10^{-7}T^2 \quad (12b)$$

$$m = 0.731 - 1.63\times10^{-4}T + 1.392\times10^{-6}T^2 - 1.151\times10^{-8}T^3 \quad (12c)$$

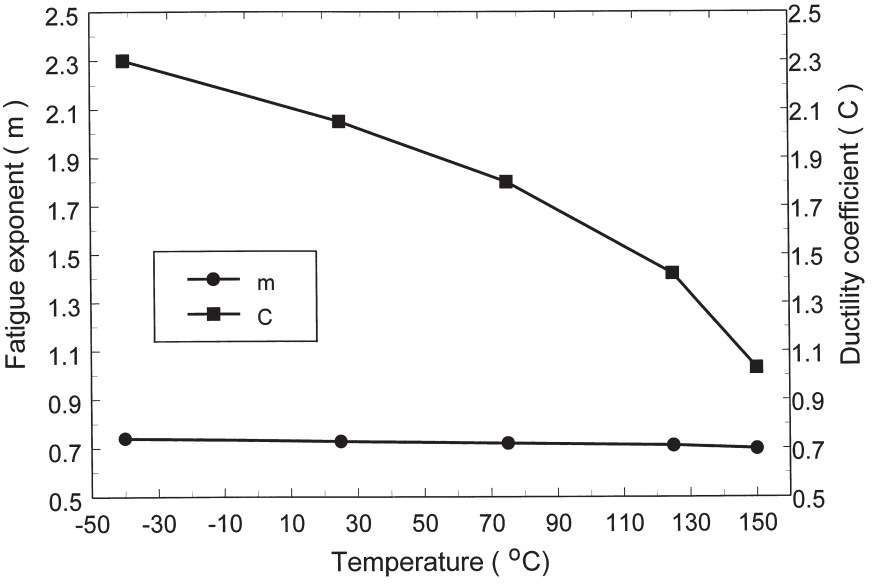


Fig. 17. Constants (m and C) in the frequency-modified Coffin–Manson model as a function of temperature.

$$C = 2.122 - 3.57\times10^{-3}T + 1.329\times10^{-5}T^2 - 2.502\times10^{-7}T^3 \quad (12d)$$

The correlation coefficient is used to measure the goodness of curve fitting in the polynomial expression. A correlation coefficient value of 1.0 represents a "perfect" fit. For the empirical formulae of k_1, k_2, m, and C, four values of 0.99628, 0.99364, 0.99505, and 0.99855 are obtained, respectively. Therefore, the formulae do represent the data accurately.

4. Conclusions

Based on the low cycle fatigue test results and analyses, the following conclusions can be made.

1. Low cycle fatigue life of eutectic solder was found to be temperature- and frequency-dependent over the range of test temperatures (from −40 to 150°C) and test frequencies (10^{-4}–1 Hz). As temperature increases, the fatigue life decreases linearly on a log–log plot. The decrease in fatigue life is small when frequency decreases from 1 to 10^{-3} Hz but becomes large when frequency reduces further from 10^{-3} to 10^{-4} Hz.
2. When the Coffin–Manson model is used to describe the low cycle fatigue behavior of 63Sn/37Pb eutectic solder alloy, the fatigue exponent m and ductility coefficient C in the model are not constant but dependent on temperature and frequency. The generalized plastic flow law was employed successfully to explain the dependence of fatigue life on temperature and frequency.
3. The frequency-modified Coffin–Manson model can be used to describe the frequency effects on the fatigue behavior of 63Sn/37Pb eutectic solder. The model given in Eq. (6) can account for the effect of test frequency on the values of the fatigue model parameters k, m, and C. However, the values of these parameters are still dependent upon test temperature. The fatigue test program conducted made it possible to derive the empirical relationship between the model parameters (k_1, k_2, m, and C) given in Equations 12a–d. This empirical formulae can be used together with the frequency-modified Coffin–Manson model given in Eq. (6) to predict the fatigue life of eutectic solder tested over the wide range of temperatures and frequencies reported in this paper.

Acknowledgements

The work reported here was carried out with the financial and technical support of Gintic Institute of Manufacturing Technology under the Upstream Project: U96-P-169. This project was done in cooperation with the School of Mechanical and Production Engineering, at Nanyang Technological University. H.L.J. Pang gratefully acknowledges the project funding and support provided through the Gintic/NTU Upstream Research program.

References

[1] Solomon HD. IEEE Trans CHMT 1986;9(4):423.
[2] Xie DJ, Chan YC, Lai JK. IEEE Trans CPMT—Part A 1996;19:669.
[3] Frear DR. IEEE Trans CHMT 1989;12:492.
[4] Solomon HD. J Electron Packag 1993;115:173.
[5] Wen LC, Ross RG. J Electron Packag 1995;117:109.
[6] Engelmaier W, Attarawala AI. IEEE Trans CHMT 1989;12:284.
[7] Guo Q, Cutiongco EC, Keer LM, Fine ME. J Electron Packag 1992;114:145.
[8] Pao YH, Govila R, Badgley S, Jih E. J Electron Packag 1993;115:1.
[9] Mei Z, Morris JW. J Electron Packag 1992;114:104.
[10] Ma YQ, Tang XY, Ma JS. J Electron Packag 1993;115:961.
[11] Guo ZF, Sprecher AF, Jung DY, Conrad H. IEEE Trans CHMT 1991;14(4):833.
[12] Sandstrom R, Osterberg JO, Nylen M. Mater Sci Technol 1993;9:811.
[13] Hong BZ, Yuan TD, Burrell L. Sensing Modeling and Simulation in Emerging Electronic Packaging 1996;17:39.
[14] Jiang H, Hermann R, Plumbridge WJ. J Mater Sci 1996;31:6455.
[15] Coffin LF. ASME Trans 1954;76:931.
[16] Manson SS. Exp Mech 1965;5:193.
[17] Solomon HD. ASTM-STP 1988;942:342.
[18] Engberg G, Larsson LE, Nylen M, Steen H. Brazing and Soldering 1986;11:62.
[19] Vaynman S, Fine ME, Jeannotte DA. Metall Trans 1988;19A:1051.
[20] Guo Z, Conrad H. J Electron Packag 1993;115:159.
[21] Solomon HD. Brazing and Soldering 1986;11:45.
[22] Morrow JD. ASTM-STP 1965;378:45.
[23] Coffin LF. ASTM-STP 1973;520:5.
[24] Shi XQ, Pang HLJ, Zhou W, Wang ZP. Scripta Mater 1999;41:289.